

High Solid-State Efficiency Fluorescent Main Chain Liquid Crystalline Polytriazoles with Aggregation-Induced Emission Characteristics

Wang Zhang Yuan,^{†,‡} Zhen-Qiang Yu,^{||} Youhong Tang,[†] Jacky W. Y. Lam,[†] Ni Xie,[†] Ping Lu,[†] Er-Qiang Chen,[§] and Ben Zhong Tang^{*,†,⊥}[†]Department of Chemistry, The Hong Kong University of Science & Technology (HKUST), Clear Water Bay, Kowloon, Hong Kong, China[‡]School of Chemistry and Chemical engineering, Shanghai Jiao Tong University, Shanghai 200240, China^{||}School of Chemistry and Chemical Engineering, Shenzhen University, Shenzhen 518060, China[§]College of Chemistry and Molecular Engineering, Peking University, Beijing 100871, China[⊥]State Key Laboratory of Molecular Neuroscience, HKUST, Clear Water Bay, Kowloon, Hong Kong, China

Supporting Information

ABSTRACT: Fluorescent liquid crystals (LCs) have wide applications in optoelectronic devices. However, the synthesis of high solid-state emission efficiency LCs is difficult. On one hand, impeding the aggregation of traditional luminogens is the prerequisite for high efficiencies; on the other hand, self-organization is an inherent attribute for LCs in the mesomorphic states. Because of such irreconcilable conflict, new strategy toward efficient fluorescent LCs is highly desirable. Herein, a conceptually new approach toward high efficiency fluorescent LCs is developed. Through rational design and combination of biphenyl-containing diazides and diynes carrying tetraphenylethylene units, soluble, regioregular, and liquid crystalline polytriazoles with high solid-state emission efficiencies (up to 63.7%) are obtained. The photophysical properties of the polymers are sensitive to their molecular structures and their solid-state quantum yields decrease with increasing spacer length. The spacer length also impacts on the mesomorphic properties. While polymers with rigid main chains exhibit nematicity, those with longer spacer lengths show better mesogenic packing and hence form smectic phases.



The photophysical properties of the polymers are sensitive to their molecular structures and their solid-state quantum yields decrease with increasing spacer length. The spacer length also impacts on the mesomorphic properties. While polymers with rigid main chains exhibit nematicity, those with longer spacer lengths show better mesogenic packing and hence form smectic phases.

INTRODUCTION

Liquid crystals (LCs) have found a wide range of high-tech applications due to their unique properties.^{1,2} For examples, they are widely used in panel display devices because of their anisotropic nature and responsiveness to electric fields.^{2,3} While ferroelectric LCs are used as temperature⁴ and pressure sensors,⁵ and are promising nonlinear optical materials,⁶ liquid crystalline semiconductors have favored potential applications in field-effect transistors,⁷ photovoltaic cells,⁸ and light-emitting diodes.⁹ Furthermore, dynamic and anisotropic liquid crystalline structures can work as low-dimensional charge,¹⁰ ion-,¹¹ and mass-transporting¹² materials.

Among various LCs, fluorescent LCs are receiving increasing attentions.^{9,13–15} The combination of intrinsic light-emitting capability and spontaneous self-organization attribute within a liquid crystalline phase is of crucial importance for optoelectronic applications, such as anisotropic light-emitting diodes and emissive liquid crystal displays.^{9,16,17} The fluorescent LCs may emit linear or circular polarized light when aligned,^{9,13g,15,17} which may be utilized for the construction of lighting and orientating layers in liquid crystal optical display devices, thus obviating the

use of polarizing sheets and absorbing color filters. The color and brightness of the light emitted by the liquid crystalline luminogens may be manipulated by external fields, which may lead to the development of readily tunable electrochromic and optical switching systems. Such approach can simplify the device design and substantially increase the device brightness, contrast, efficiency, and viewing angle.^{3,18}

Despite the promising prospects of high emission efficiency LCs, their synthesis is intractable. In the mesophases, particularly those formed by disk-like molecules,^{13c} the chromophoric mesogens are regularly packed and undergo strong intermolecular interactions, which often quench their light emissions due to the formation of detrimental species such as excimers and exciplexes.^{13g,19–21} The light emission is often enhanced with the sacrifice of molecular packing, thus making the synthesis of efficient fluorescent LCs a daunting task.

Received: September 30, 2011

Revised: November 10, 2011

Published: November 22, 2011

Our group is interested in creating molecular and polymeric LCs.²² We have synthesized a wide variety of side chain liquid crystalline polyacetylenes carrying chromophoric and mesogenic pendants. Some of which can emit intensely in the condensed phase.^{23,24} Recently, we discovered a novel phenomenon of aggregation-induced emission (AIE) in some propeller-shaped molecules.^{25,26} Instead of quenching commonly observed in “conventional” luminophors, aggregation has enhanced their light emission, turning them from weak fluorophors into strong emitters. Introduction of AIE-active dyes into liquid crystals may solve such the above problem but such attempt has rarely reported.

Tetraphenylethylene (TPE) is a typical AIE-active dye.^{26,27} It is nonemissive in dilute solution because its active intramolecular rotations effectively dissipates the energy of its excitons through nonradiative pathways. On the contrary, it emits intensely in the aggregate state due to the physical restriction of its intramolecular rotations. Polymers containing TPE units are thus expected to show AIE phenomenon.²⁸ Meanwhile, the polymers can be imparted with mesomorphic properties through rational molecular design. Herein, we present our effort on the creation of AIE-active liquid crystalline polymers (AIE-LCPs). The copper-catalyzed 1,3-dipolar cycloaddition of alkynes with azides is a typical example of “click reaction”. Since the reaction enjoys the advantages of mild reaction conditions, high efficiency and regioselectivity, and simple purification procedures, it has

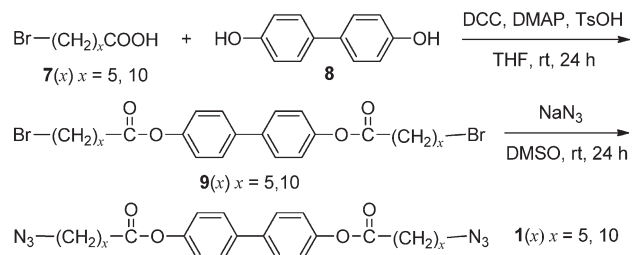
become a versatile synthetic tool with applicability in diverse areas.^{29–31} In this paper we adopted such methodology for the preparation of new polymers. All the synthesized polytriazoles are both AIE-active and liquid crystalline. Their solid-state quantum efficiencies range from 24.5 to 63.7%, which are much higher than those of reported luminescent liquid crystals.^{15b,20} The effects of spacer length on their emission efficiency and mesomorphic behaviors are also discussed.

EXPERIMENTAL SECTION

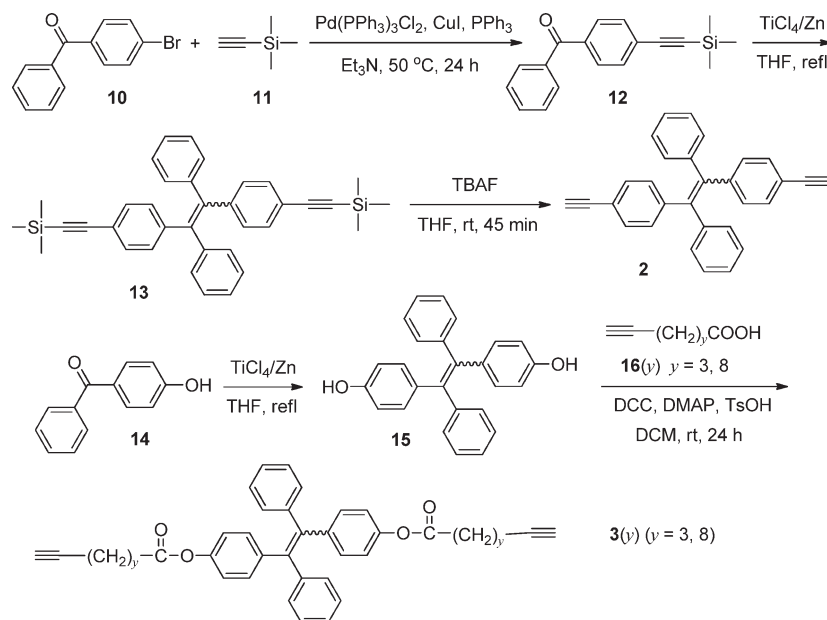
Materials. THF was distilled under normal pressure from sodium benzophenone ketyl under nitrogen immediately prior to use. Dichloromethane (DCM) was distilled under normal pressure over calcium hydride under nitrogen before use. Triethylamine (TEA) was distilled and dried over potassium hydroxide. *p*-Toluenesulfonic acid monohydrate (TsOH), *N,N'*-dicyclohexylcarbodiimide (DCC), 4-dimethylaminopyridine (DMAP), 6-bromohexanoic acid [7(5)], 11-bromoundecanoic acid [7(10)], 4,4'-biphenol (8), 4-bromobenzophenone (10), (trimethylsilyl)acetylene (11), 4-hydroxybenzophenone (14), copper(I) iodide (CuI), triphenylphosphine (PPh₃), dichlorobis(triphenylphosphine)palladium(II) [Pd(PPh₃)₂Cl₂], titanium tetrachloride (TiCl₄), zinc dust, 1 M tetrabutylammonium fluoride (TBAF) in THF (containing 5% water) were all purchased from Aldrich and used as received. Catalysts Cu(PPh₃)₃Br and Cp^{*}Ru(PPh₃)₂Cl were prepared according to the literature methods.³²

Instrumentations. ¹H and ¹³C NMR spectra were measured on a Bruker ARX 400 spectrometer using chloroform-*d* or DMSO-*d*₆ as solvent and tetramethylsilane (TMS) as internal standard. Matrix-assisted laser desorption/ionization time-of-flight (MALDI-TOF) high-resolution mass spectra (HRMS) were recorded on a GCT premier CAB048 mass spectrometer. Absorption spectra were taken on a Milton Roy Spectronic 3000 Array spectrometer. Emission spectra were taken on a Perkin-Elmer spectrofluorometer LS 55. The quantum yields (Φ_F's) of the polymers in THF solutions were estimated using quinine sulfate (Φ_F = 54% in 0.1 M H₂SO₄) as standard, while those of the solid films were determined using an integrating sphere. The films were prepared by casting the polymer solutions (5 mg/mL in chloroform, THF, 1,2-dichloroethane or DMF) at ambient conditions. The films

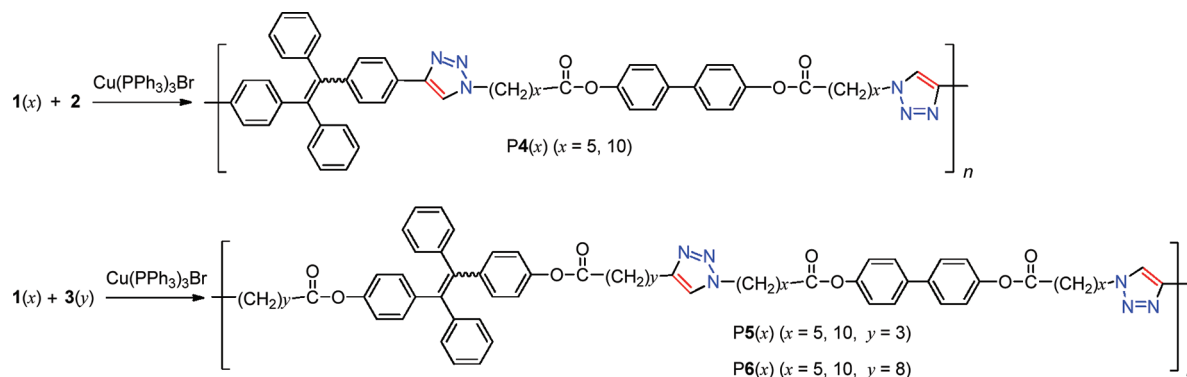
Scheme 1



Scheme 2



Scheme 3



were stood overnight at room temperature before measurement. Molecular weights (M_w and M_n) and polydispersity indexes (M_w/M_n) of the polymers were estimated by a Waters Associates gel permeation chromatography (GPC) system in THF. A set of monodisperse polystyrene standards covering molecular weight range of 10^3 – 10^7 was used for the molecular weight calibration.

The thermal stability of the polymers was evaluated on a Perkin-Elmer TGA 7 under nitrogen at a heating rate of $20\text{ }^\circ\text{C}/\text{min}$. A Perkin-Elmer DSC 7 was employed to measure the phase transition thermograms. An Olympus BX 60 polarized optical microscope (POM) equipped with a Linkam TMS 92 hot stage was used to observe the anisotropic optical textures. One-dimensional wide-angle X-ray diffraction (1D-WAXD) powder experiments were performed on a Philips X'Pert Pro diffractometer with a 3 kW ceramic tube as the X-ray source ($\text{Cu K}\alpha$) and an X'celerator detector. The sample stage was set horizontally and the samples were protected by nitrogen gas during the measurements. The reflection peak positions were calibrated with silicon powder ($2\theta > 15^\circ$) and silver behenate ($2\theta < 10^\circ$). Background scattering was recorded and subtracted from the sample patterns. A temperature control unit (Paar Physica TCU 100) in conjunction with the diffractometer was utilized to study the structure evolutions as a function of temperature.

RESULTS AND DISCUSSION

Monomer Preparation. With a view to synthesize AIE-LCPs by click reaction, we prepared biphenyl-containing diazides with different aliphatic spacer lengths according to Scheme 1. We first esterified 4,4'-biphenol (**8**), with ω -bromoalkanoic acid **7(x)** in the presence of DCC, DMAP, and TsOH. The resulting compounds **9(x)**, were then reacted with sodium azide, furnishing the desirable products **1(x)**.

We also synthesized TPE-functionalized diynes **2** and **3(y)**, according to the synthetic routes shown in Scheme 2. To obtain compound **2**, we first prepared compound **12** by palladium-catalyzed cross-coupling of 4-bromobenzophenone (**10**) with trimethylsilylacetylene (**11**). McMurry coupling of **12** catalyzed by TiCl_4 and Zn afforded **13**, which converted into **2** by cleavage of its trimethylsilyl groups in basic medium. Diynes **3(y)** are structural congeners of **2** but their triple bond functionalities are connected to the TPE core through alkyl chains and ester groups. They were synthesized by McMurry coupling of 4-hydroxybenzophenone (**14**) followed by esterification with β -alkynoic acids **16(y)**. All the reactions proceeded smoothly and the desirable monomers were obtained in high yields. The monomers were characterized by standard spectroscopic methods, from which

Table 1. Click Polymerizations of Diazides with Diynes^a

no.	solvent	time (h)	yield (%)	M_w^b	M_w/M_n^b
1(5) + 2					
1	THF	12	85.1	11 800 ^c	1.42
2	DMF	12	94.1	11 800 ^c	1.66
3	THF	6	40.0	3400	1.30
4 ^d	THF	12	94.0	4900	1.61
1(5) + 3(3)					
5	THF	12	63.7	8900	1.67
6	DMF	12	97.1	11 400	1.91
1(5) + 3(8)					
7	THF	12	75.2	16 200	2.00
8	DMF	12	79.3	10 200	1.77
1(10) + 2					
9	THF	12	94.5	14 800	1.48
10	DMF	12	94.8	14 600	1.47
1(10) + 3(3)					
11	THF	12	87.0	12 900	1.72
12	DMF	12	90.4	12 900	1.76
1(10) + 3(8)					
13	THF	12	63.6	11 900	1.61
14	DMF	12	85.4	12 900	1.62

^a Carried out at $60\text{ }^\circ\text{C}$ under nitrogen using $\text{Cu}(\text{PPh}_3)_3\text{Br}$ as catalyst unless otherwise specified. ^b Estimated by GPC in THF on the basis of a polystyrene calibration. ^c THF soluble fraction. ^d $\text{Cp}^*\text{Ru}(\text{PPh}_3)_2\text{Cl}$ was used as catalyst.

satisfactory analysis data corresponding to their molecular structures were obtained (see Supporting Information for details).

Click Polymerization. We then carried out the polycycloaddition reactions of **1(x)** with **2** and **3(y)** according to Scheme 3. We first tried to polymerize **1(5)** and **2** by $\text{Cu}(\text{PPh}_3)_3\text{Br}$, an effective organosoluble catalyst for the 1,4-regioregular 1,3-dipolar cycloaddition.^{29,31} Reaction conducted in THF at $60\text{ }^\circ\text{C}$ for 12 h gives some THF-insoluble products, which can dissolve readily in DMF. After precipitation of the solution into hexane/THF mixture, **P4(5)** is isolated in a yield of 85.1% (Table 1, no. 1). The M_w and M_w/M_n of its THF soluble fraction are 11 800 and 1.44, respectively. The mixture remains homogeneous throughout the polymerization process when the polymerization is carried out in

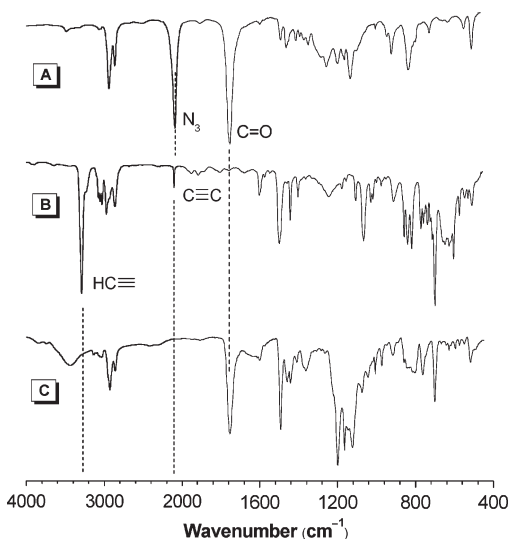


Figure 1. IR spectra of (A) monomer 1(S), (B) monomer 2, and (C) their polymer P4(S) (sample taken from Table 1, no. 2).

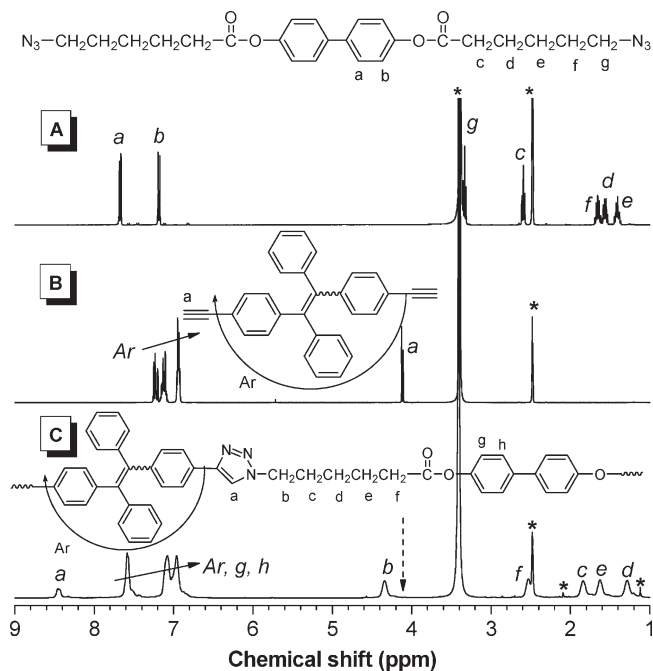


Figure 2. ^1H NMR spectra of (A) monomer 1(S), (B) monomer 2, and (C) their polymer P4(S) (sample taken from Table 1, no. 2) in $\text{DMSO}-d_6$ at room temperature. The solvent peaks are marked with asterisks.

DMF. Although a higher yield is obtained, the polymer is soluble only in DMF and DMSO but dissolves partially in THF, DCM, and chloroform. The limited solubility of the polymer should be ascribed to the rigidity of the polymer chain and its higher molecular weight. We thus fine-tuned the molecular weight of the polymer by lowering the reaction time to 6 h and obtained completely soluble products albeit in a low yield. Previously, it is found that ruthenium catalysts can produce polymers with better solubility due to the formation of more twisted 1,5-triazole units.³³ When $\text{Cp}^*\text{Ru}(\text{PPh}_3)_2\text{Cl}$ was used as catalyst for the polymerization

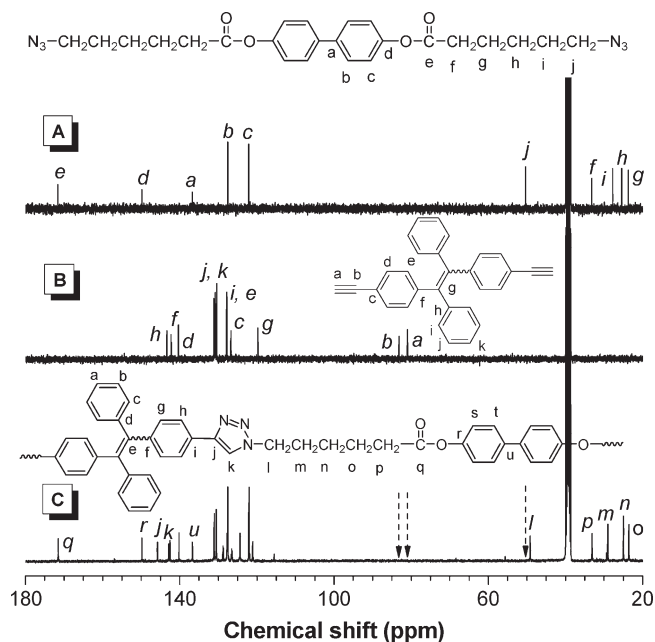


Figure 3. ^{13}C NMR spectra of (A) monomer 1(S), (B) monomer 2, and (C) their polymer P4(S) (sample taken from Table 1, no. 2) in $\text{DMSO}-d_6$ at room temperature.

of 1(S) and 2, a soluble polymer is isolated in high yield but rather low molecular weight (Table 1, no. 4).

The polymerizations of other monomer pairs are conducted using $\text{Cu}(\text{PPh}_3)_3\text{Br}$ as catalyst in THF or DMF. As depicted in Table 1, nos. 5–14, all the polymers are obtained in high yields (63.6–97.1%) with moderate M_w values of 8 900–16 200. Generally, the polymerizations performed in DMF give much higher yields than those conducted in THF. Thanks to their long alkyl chains, P5(x) and P6(x) possess good solubility in THF, DCM, and chloroform.

Structural Characterization. All the polymers are characterized by spectroscopic techniques and give satisfactory analysis data corresponding to their expected structures. An example of the IR spectrum of P4(S) is shown in Figure 1. The spectra of its monomers 1(S) and 2 are also given in the same figure for comparison. Monomer 1(S) shows absorption band at 2096 cm^{-1} due to the stretching vibration of its azido functionality. The $\text{HC}\equiv$ and $\text{C}\equiv\text{C}$ stretching vibrations of monomer 2 are observed at 3276 and 2107 cm^{-1} . After polymerization, all these are absent in the spectrum of P4(S), indicating that all the azido groups of 1(S) and triple bonds of 2 have been consumed by polycycloaddition.

We further characterized the polymers by NMR spectroscopy. Figure 2 shows the ^1H NMR spectra of monomers 1(S) and 2, and their corresponding polymer P4(S) in $\text{DMSO}-d_6$. The polymer gives no peaks corresponding the proton adjacent to the azido group of 1(S) and acetylenic proton of 2 at $\delta \sim 3.3$ and ~ 4.1 , respectively (Figure 2, parts A and B). Meanwhile, new resonances assigned to the absorptions of the olefin proton of 1,4-disubstituted triazole ring and its neighboring methylene protons are emerged at $\delta \sim 8.5$ and $\delta \sim 4.3$. No olefin proton resonance associated with 1,5-disubstituted is detected and all the peaks can be readily assigned, suggesting that the polymeric product is indeed P4(S) with molecular structure as shown in Figure 2C.

Figure 3 shows the ^{13}C NMR spectrum of polymer P4(5) along with those of monomer 1(5) and 2. While the methylene

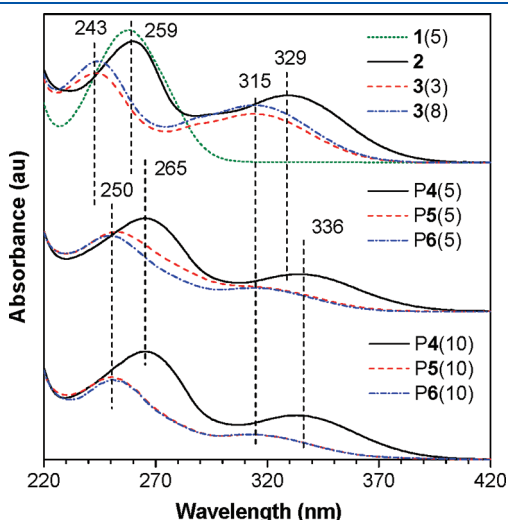


Figure 4. Absorption spectra of monomers and polymers in THF. Concentration: 2×10^{-5} M (monomers); 0.008 mg/mL (polymers). Soluble fraction of P4(5) in THF was used for the measurement.

carbon next to the azido group of 1(5) resonates at δ 50.31 (Figure 3A), the absorptions of the acetylenic carbons of 2 occur at δ 83.14 and 80.88 (Figure 3B). The spectrum of P4(5) shows no these absorptions but new peaks associated with the resonances of the olefin carbons at δ 145.81 and 142.76. This result testifies that the azido groups of 1(5) and triple bonds of 2 have been cyclized into triazole rings in P4(5), which well agrees with those from the IR and ^1H NMR analyses.

Electronic Transitions. Figure 4 shows the absorption spectra of the monomers and polymers in THF. The biphenyl pendant of 1(5) absorbs at 257 nm, while the absorption of the TPE moiety of monomer 2 occurs at 259 and 329 nm. After polymerization, their corresponding polymer P4(5) absorbs at slightly longer wavelengths of \sim 265 and 336 nm. Clearly, the polymer is more conjugated because of electronic communication between the TPE unit and the newly formed triazole rings. Because of the structural similarity, polymer P4(10) shows an absorption profile identical to that of P4(5). The UV spectra of P5(x) and P6(x) are similar, featuring two maximum at 250 and 315 nm. Their spectra patterns are resembled to those of 3(y) because their triazole rings are well separated from the TPE units by long alkyl spacers, which have hampered their electronic interactions.

Aggregation Induced Emission. TPE is a well-known AIE luminogen and it is thus anticipated that our TPE-containing

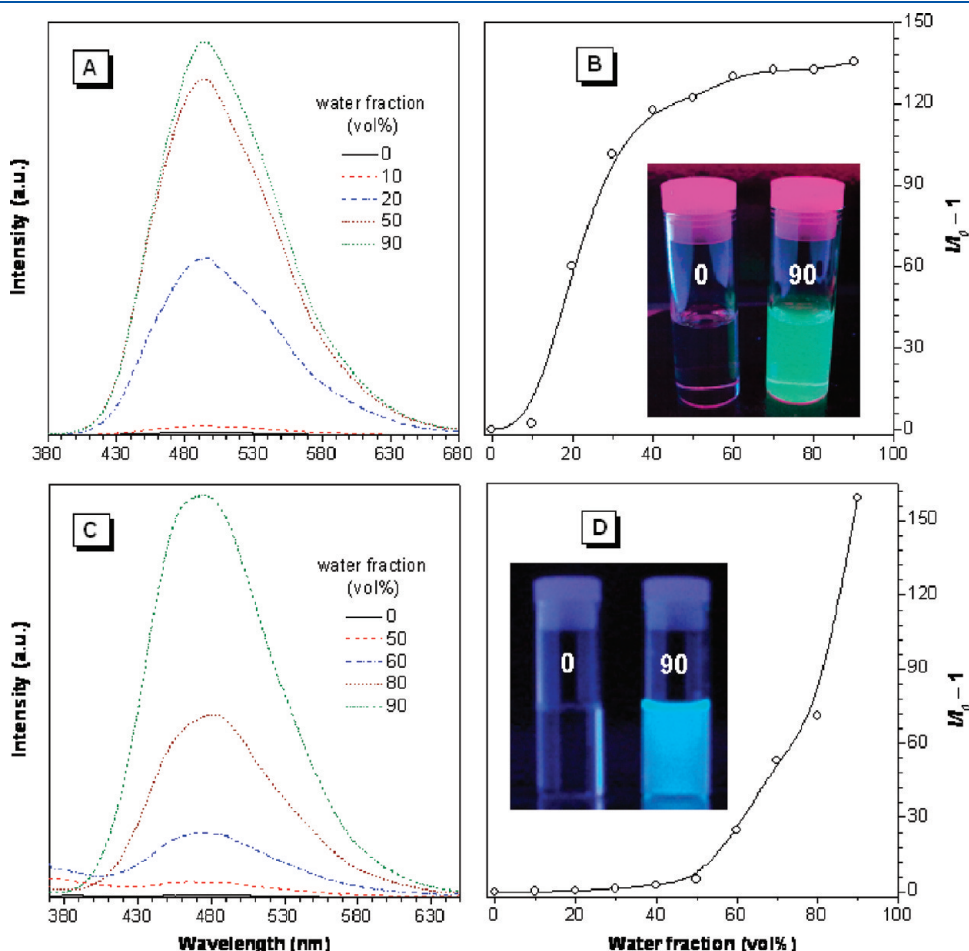


Figure 5. Emission spectra of (A) P4(5) in DMF/H₂O and (C) P6(5) in THF/H₂O mixtures with varied water fractions. Plots of $(I/I_0 - 1)$ values versus water fractions of the aqueous mixtures at (B) 493 and (D) 475 nm for P4(5) and P6(5), respectively. Photos of P4(5) and P6(5) in DMF and THF with 0 and 90% water contents taken under UV light, respectively, are given in panels B and D. Concentration (mg/mL): 0.044 [P4(5)], 0.06 [P6(5)]. Excitation wavelength (nm): 350 [P4(5)]; 340 [P6(5)].

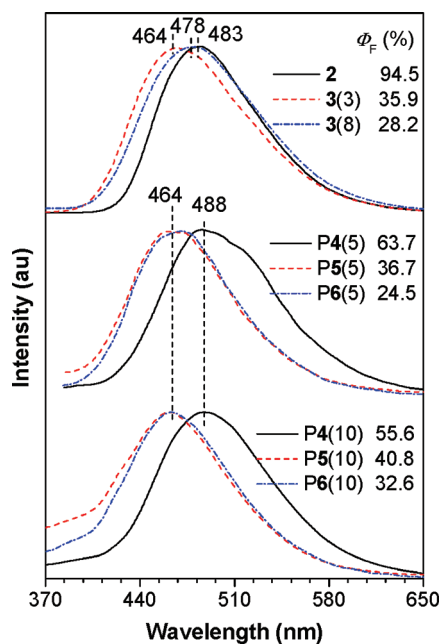


Figure 6. Emission spectra of thin films of monomers **2**, **3(3)**, **3(8)**, and polymers **P4(x)**, **P5(x)**, and **P6(x)** at room temperature. Films were cast from corresponding CHCl_3 solutions (5 mg/mL). Excitation wavelength: 350 nm. Quantum yields of the polymers in THF: 0.67% [**P4(5)**], THF-soluble fraction], 0.51% [**P5(5)**], 0.28% [**P6(5)**], 0.19% [**P4(10)**], 0.20% [**P5(10)**], and 0.26% [**P6(10)**].

polymers are also AIE-active. To confirm this, we investigate their emission behaviors in solvent/nonsolvent mixtures. As shown in Figure 5A, polymer **P4(5)** is almost nonluminescent in pure DMF. Addition of water into its DMF solution, has, however, enhanced its light emission. The higher the water content, the stronger is the light emission. In 90% aqueous mixture, the emission intensity is >135-fold higher than that in the pure DMF solution, exhibiting a bright emission with its maximum at 493 nm (Figure 5B). Since biphenyl emits in the UV region, the visible emission of **P4(5)** should be, in most cases, originated from its TPE chromophoric units. The photographs depicted in the inset exemplify the nonemissive and strongly luminescent nature of the DMF solution and 90% aqueous mixtures. Clearly, the AIE characteristics of the TPE units are preserved when they are incorporated into polymer. Polymer **P6(5)** also exhibits typical AIE behavior. As can be seen in Figures 5C and 5D, the polymer emits no light in THF but gives a strong sky-blue emission at 475 nm when aggregated in the aqueous mixture. The emission is gradually intensified with increasing water content in the THF/water mixture. At 90% water content, the intensity is more than 159-fold higher than that in pure THF solution. Similar phenomenon are also observed in **P4(10)**, **P5(x)**, and **P6(10)** (Figures S1–S4, Supporting Information). In their 90% aqueous mixtures, the emission intensities are >150-fold higher than those in pure THF.

We also investigated their photophysical properties in the solid state. Thanks to the AIE effect of the TPE units, the bulk solids of the **P4(x)**, **P5(x)**, and **P6(x)** are highly emissive under UV light illumination (Figure S5, Supporting Information). The polymer films are also capable of emitting light intensely. Figure 6 depicts their emission spectra; for comparison, the spectra of their monomers **2** and **3(y)** are also given in the same figure. Since **P4(5)** and **P4(10)** possess higher conjugation, they emit at

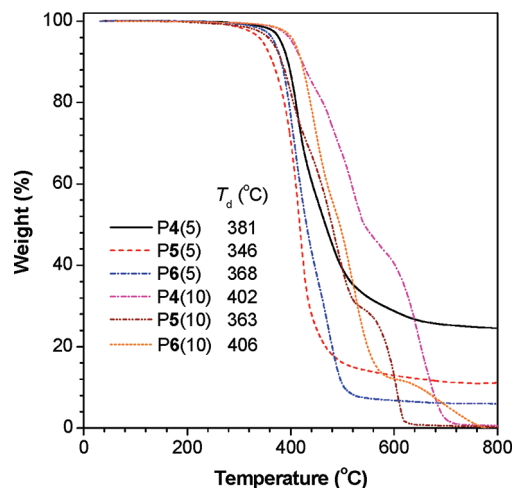


Figure 7. TGA thermograms of **P4(x)**, **P5(x)**, and **P6(x)** measured under nitrogen at a heating rate of 20 °C/min.

slightly longer wavelengths (~ 488 nm) than **2** (483 nm). The emission maxima of **P5(x)** are located at wavelengths similar to that of **3(3)**. Those of **P6(x)** are, however, blue-shifted from **3(8)** by 14 nm. The relative longer alkyl spacers in **P6(x)** may have effectively hampered the interactions between the TPE units, thus resulted in emission at the bluer region.

To have a quantitative comparison, the quantum yields (Φ_F 's) of the polymers in THF solutions and solid film states are measured. The Φ_F values in solutions are quite low. Those of their solid films are, however, much higher and ranged from 24.5 to 63.7%. Closer inspection reveals that Φ_F values of the monomers and polymers are varied by the spacer length. For example, when the methylene unit is progressively increased from **P4(5)** to **P5(5)** and then **P6(5)**, the quantum yield decreases from 63.7% to finally 24.5%. Thus, the incorporation of electronically saturated alkyl chains in the monomers and polymers are harmful to their light emissions, presumably due to the obstruction of the TPE aggregation formation.

Thermal Stability. Formation of mesophases of thermotropic liquid crystals is realized by the application of heat, the thermal stability of the polymers is thus of primary concern. Figure 7 gives the TGA thermograms of the polymers recorded under nitrogen. All the polymers show high resistance to thermolysis, with 5% weight loss (T_d) occurring from 346 to 406 °C. The T_d values are much higher than that of polystyrene (330 °C), a stable commodity polymer.³⁴ The high thermal stability of the polymers renders them useful for practical applications.

Mesomorphism. After checking the thermal stability of the polymers, we investigated their mesomorphic properties. As monomers **1(5)** and **1(10)** contain mesogenic biphenyl unit, we first checked whether they are liquid crystals. Figure 8 shows the DSC thermograms of **1(5)** and **1(10)** recorded during the first cooling and second heating processes, while their POM textures observed on cooling from their isotropic liquids are given in Figure 9.

During the first cooling cycle, **1(5)** shows three exothermic peaks at 88.6, 7.8, and 3.7 °C. POM observation reveals that upon cooling **1(5)** from the isotropic state (i) to 94.2 °C, typical mosaic texture of smectic B phase (S_B) with lancet³⁵ emerges from the homotropic dark background. More anisotropic domains appear at 92.8 °C and their sizes grow bigger when the temperature is further lowered (Figure 9A). The transition peaks at 7.8 and

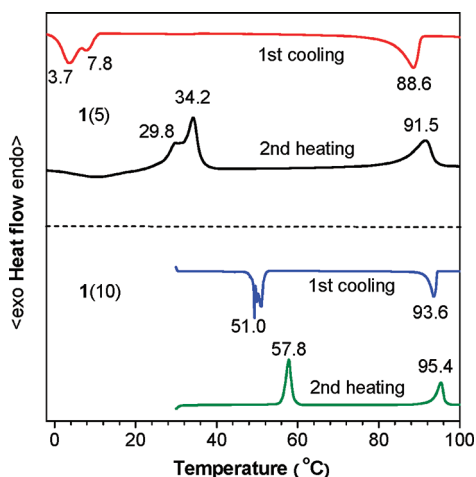


Figure 8. DSC thermograms of monomers **1(5)** and **1(10)** recorded under nitrogen during the first cooling and second heating cycles with a scan rate of 10 °C/min.

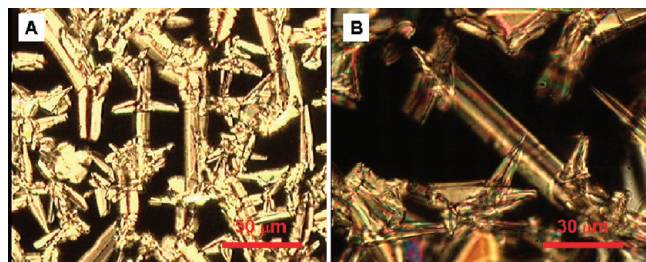


Figure 9. Mesomorphic textures observed on cooling (A) **1(5)** to 92.8 °C and (B) **1(10)** to 95.4 °C from their isotropic states at a cooling rate of 0.5 and 0.2 °C/min, respectively.

3.7 °C are ascribed to S_B -crystal (k) and k - k transitions, respectively. The DSC curve recorded in the second heating cycle is the mirror image of that obtained in the first cooling scan, three endothermic peaks corresponding to the k - k , k - S_B , and S_B - i transitions are detected at 29.8, 34.2, and 91.5 °C, respectively.

1(10) is the congener of **1(5)** with much longer flexible spacers and it is of interest to study how it behaves mesomorphically. As depicted in Figure 8, during the first cooling cycle, **1(10)** shows two distinct transition peaks at 93.6 and 51.0 °C. When it is cooled from its isotropic state to 95.4 °C, mosaic texture of S_B mesophase with lancet similar to that of **1(5)** is observed. The second heating scan detects two endothermic peaks at 57.8 and 95.4 °C, which are associated with the k - S_B and S_B - i transitions, respectively.

To gain more information on the monomer packing arrangements in the mesophases, 1D-WAXD measurements were carried out. The diffractograms of **1(5)** and **1(10)** obtained at 100 °C display only diffuse halos at high-angle region, indicative of their isotropic feature (Figure 10). When **1(5)** is cooled to 90 °C, two sharp peaks at $2\theta = 2.99$ and 19.83° are recorded. The d -spacing derived from the former peak is 29.53 Å, which is comparable to the fully extended molecular length of **1(5)** ($l = 31.63$ Å). The peak at $2\theta = 19.83^\circ$ has quite a narrow full width at half-maximum of 0.326°. Such results suggest that long-range order is present within the smectic layer, which is typical characteristic of the S_B mesomorphic phase.

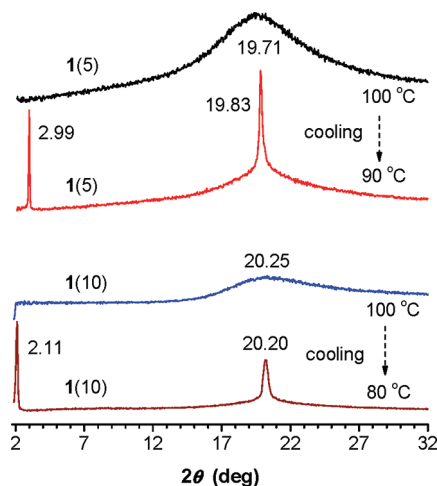


Figure 10. X-ray diffraction patterns of **1(5)** and **1(10)** obtained on cooling from their isotropic liquids.

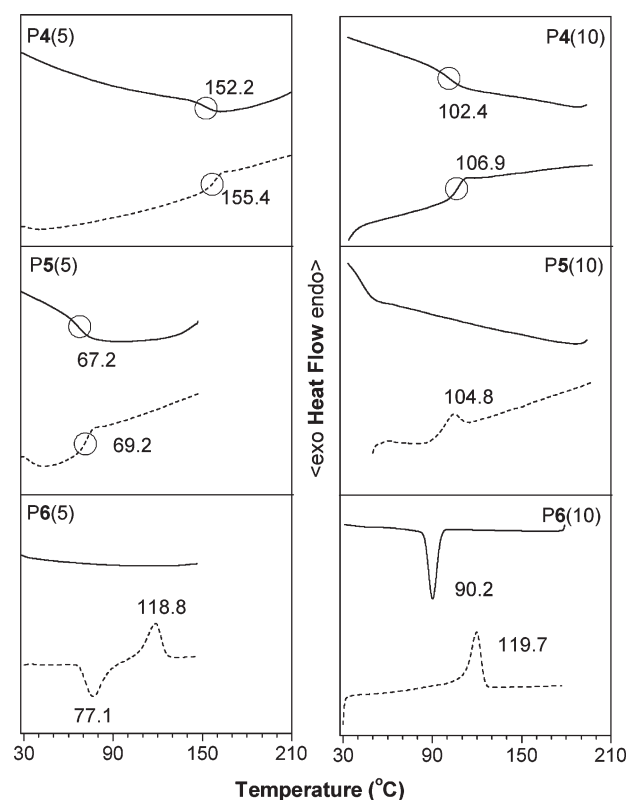


Figure 11. DSC thermograms of the polymers recorded under nitrogen during the first cooling (solid line) and second heating (dash line) cycles at a scan rate of 10 °C/min.

Similar WAXD pattern is observed in **1(10)** when it is cooled to 80 °C. The reflection at $2\theta = 20.20^\circ$ gives the average distance of the shorter preferred spacing ($d = 4.39$ Å) occurring in the lateral packing arrangement of the mesogens. The layer spacing derived from the peak at 2.11° is 41.84 Å, which well approaches to the molecular length of **1(10)** ($l = 44.07$ Å) at its most extended conformation. All these features confirm the formation of S_B phase.

We then continued our study on the mesomorphic properties of the polymers. We first checked the thermal transitions of the

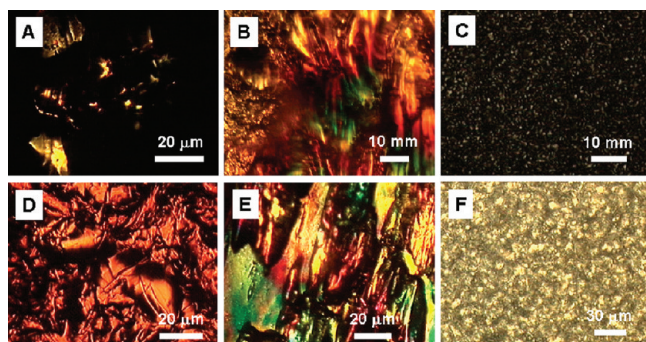


Figure 12. Mesomorphic textures observed on cooling (A) P4(5) to 159.9 °C, (B) P5(5) to 89.9 °C, (C) P6(5) to 94.9 °C, (D) P4(10) to 250.6 °C, (E) P5(10) to 69.8 °C, and (F) P6(10) to 114.9 °C from their melting states at a cooling rate of 1 °C/min. Photos in parts A, B, D, and E are taken after application of a shearing force.

polymers by DSC. In the first cooling cycle, P4(5), P4(10), and P5(5) exhibit discontinuities in the heat capacity at 152.2, 102.4, and 67.2 °C (Figure 11), respectively, associated with the glass transitions of the polymer chains. The corresponding transitions in the second heating scan are observed at 155.4, 106.9, and 69.2 °C, respectively. For P5(10), while no obvious peak is observed in the first cooling process, a weak diffusion transition peaked at 104.8 °C is observed, which may be resulted from a close overlap of an exothermic peak of chain rearrangement and an endothermic peak of a LC–i phase transition.

Unlike to those observed for P4(*x*) and P5(*x*), the thermograms of P6(*x*) show distinct sharp peaks, which are usually associated with first order phase transitions. As depicted in Figure 11, the thermogram of P6(5) recorded in the first cooling cycle is basically a flat line parallel to the abscissa. On the contrary, during the second heating cycle, two peaks related to chain rearrangement and LC-i transition are observed at 77.1 and 118.8 °C, respectively. For those of P6(10), sharp peaks at 90.2 and 119.7 °C are recorded during the first cooling and second heating circles, which are corresponded to the i-LC and LC-i transitions, respectively.

No birefringences are observed when P4(*x*) and P5(*x*) are cooled from their melted states. Anisotropic domains are, however, emerged under shearing (Figure 12, parts A, B, D, and E). Thus, all the polymers are mesomorphic. The liquid crystalline domains of the polymers are too small to be observed without external stimuli. Such phenomenon should be caused by the high rigidity of the main chain, which impedes the packing arrangements of the mesogenic units. When a shear force is applied, the small domains merge together and aligned along the shear direction, thus them observable under POM.

Thanks to the relative longer flexible spacers in P6(5) and P6(10) which render the mesogenic units more freedom to pack, small entities are emerged from the homotropic dark background when their isotropic liquids are cooled. The entities grow bigger upon cooling but their development into a typical texture seems to be a difficult task. We attempted to grow such bigger LC domains with care but failed to obtain any characteristic texture.

We carried out 1D-WAXD experiments of the polymers at different temperatures in order to gain more information concerning their molecular arrangements, and modes of packing in the mesophases. As shown in Figure 13A, the diffractogram of thin film of P4(10) cast from its THF solution at 40 °C shows a

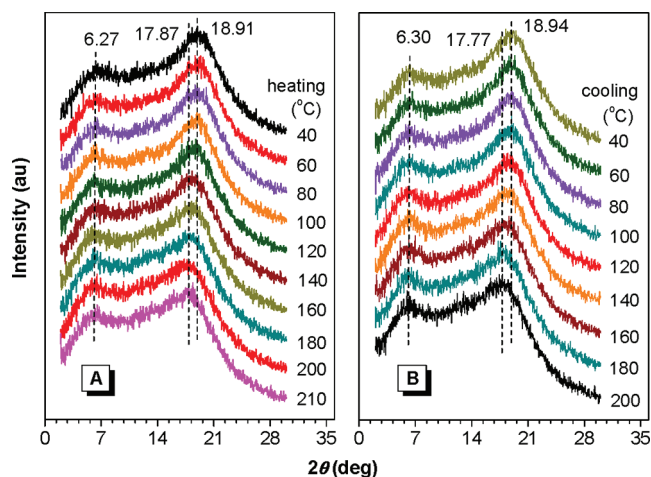


Figure 13. X-ray diffractograms of P4(10) at different temperatures obtained during the (A) heating and (B) cooling cycles.

broad peak at $2\theta = 6.27^\circ$ and a halo at 18.91° . The spectral profile keeps almost unchanged when the polymers is heated to temperatures up to 210 °C, which is much higher than the glass transition temperature (T_g). The diffractogram also changes little upon cooling (Figure 13B). It indicates that the film formed from the solution is liquid crystalline and the mesophase is stable during both heating and cooling processes. To some degree, this result is similar to those observed in Zhou's mesogen-jacketed liquid-crystalline polymers, in which the mesomorphic phases are stable at both elevated and low temperatures.³⁶ It is in some sense understandable when we take the high stiffness of the polymer main chain into consideration. The rigid polymer strand hampers the packing of the mesogenic units but on the other hand, stabilizes and fixes their alignment. The *d*-spacing associated with the diffuse halo changes at temperatures higher than T_g , which is commonly observed in LCs exhibiting nematicity.³⁷ According to its poor packing feature and temperature-dependent *d*-spacing phenomenon, we can assign the mesomorphic phase of P4(10) to be nematic.

When three more methylene units are introduced into P4(10), the resultant polymer P5(10) shows better mesogenic packing. Its X-ray diffractograms measured at different temperatures during the heating and cooling cycles are depicted in Figure 14. At 40 °C, the diffractogram shows three reflection peaks at $2\theta = 3.93, 8.30, 20.48^\circ$ and a diffuse halo at 18.40° , from which *d*-spacings of 22.46, 10.64, 4.32, and 4.82 Å are derived, respectively (Figure 14A). The *d*-spacings of the former two peaks is close to 2:1, meanwhile the peak in the high angle region is relatively narrow, thus indicating the formation of smectic phase and relatively ordered molecular packing within the layer. The peaks in low angle region become weaker at elevated temperatures and disappear completely at 110 °C, which is associated with the LC-i transition and consistent with the DSC result. Meanwhile, in the high angle region, the peaks become broader and weaker and only the diffuse halo remained. In the subsequent cooling process from 150 to 40 °C, no observable change is observed in the diffractograms. This indicates that the ordered mesogenic packing lost in the heating scan cannot be recovered by subsequent cooling process due to the low chain mobility caused by the still rigid polymer strand.

Polymer P6(10) has even longer flexible spacers than that of P5(10), and its temperature-variable WAXD diagrams are shown

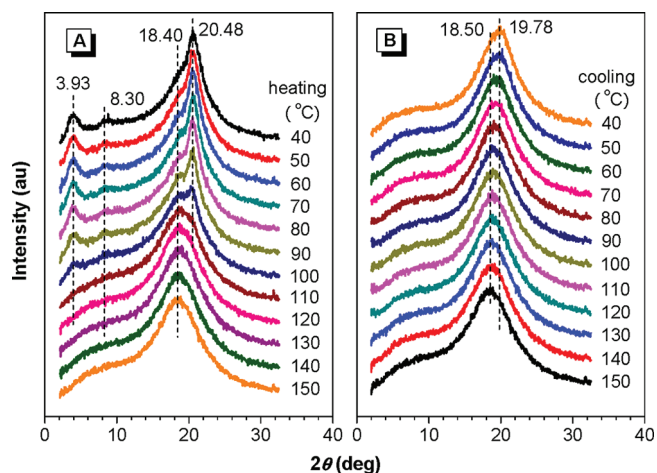


Figure 14. X-ray diffractograms of P5(10) at different temperatures obtained during the (A) heating and (B) cooling cycles.

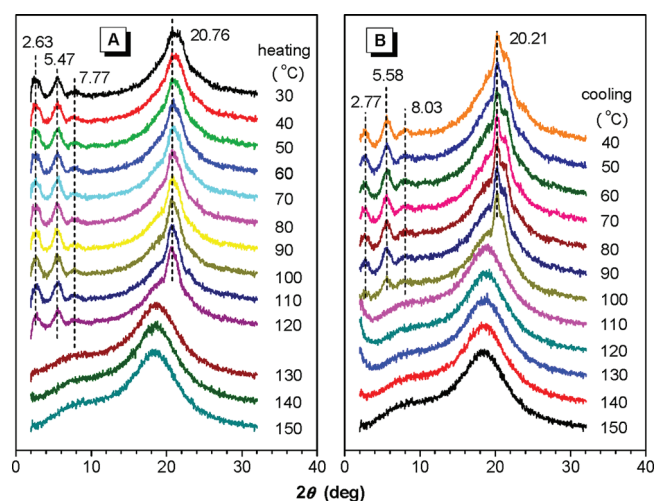


Figure 15. X-ray diffractograms of P6(10) at different temperatures obtained during the heating and cooling cycles.

in Figure 15. At 30 °C, three peaks and one diffuse halo at $2\theta = 2.63, 5.47, 7.77,$ and 20.76° are observed. When the sample is heated to 130 °C, the former three reflections disappear, revealing that the isotropic state is reached and the mesogens are now randomly orientated. These peaks, are, however, emerged again upon cooling (Figure 15B), thanks to the relative more flexible chain of P6(10), which provides little constraint for the mesogens to pack in the mesophase. From the XRD profile, it is reasonable to assign its mesogenic phase as smectic. For detailed phase identification, further investigation on its molecular packing is required and is actively undergone in our laboratory. Other WAXD measurement result for P4(S), P5(S), and P6(S) are given in Figures S6–S8, Supporting Information. No obvious signals at low angles are recorded, suggesting that all the polymers exhibit nematicity at high temperature.

CONCLUSIONS

In this paper, regioselective 1,3-dipolar polycycloadditions of biphenyl-containing diazides and tetraphenylethene-carrying diynes are initiated by $\text{Cu}(\text{PPh}_3)_3\text{Br}$ in THF or DMF generating

soluble polytriazoles in high yields (up to 97.1%) narrow molecular weight distributions.

All the polymers are AIE-active. While they emit weakly in solutions with Φ_F values not more than 0.67%, they become strong emitters in the aggregated states with Φ_F values up to 63.7%. The Φ_F value is sensitive to the spacer length and decreases when the ethylene unit in the polymers becomes higher.

All the polymers enjoy high thermal stability and are liquid crystalline. While polymers P4(x) possess rigid main chains and thus exhibit nematicity, their counterparts with longer spacer lengths, i.e., P5(x) and P6(x), show better mesogenic packing and may form smectic phases. Our results have shown that through rational design, it is feasible to create liquid crystals with strong light emissions. We are currently working on the synthesis of new mesomorphic polymers and studied their polarized emission. Details will be published in a separate paper.

ASSOCIATED CONTENT

S Supporting Information. Synthetic procedures and characterization data of the polymers and monomers, emission spectra of P4(10), P5(5), P5(10), and P6(10) in THF/water mixtures, photographs of the polymer powders taken under normal room and 365 nm UV illumination, schematic illustration of the molecular length of **1**(x) in their fully extended conformations, XRD diffractograms of P4(5), P5(5), and P6(5), and emission spectra of different P6(5) and P6(10) films. This material is available free of charge via the Internet at <http://pubs.acs.org>.

AUTHOR INFORMATION

Corresponding Author

*Telephone: +852-2358-7375. Fax +852-2358-1594. E-mail tangbenz@ust.hk

ACKNOWLEDGMENT

We thank the support from the Research Grants Council of Hong Kong (603509, HKUST2/CRF/10, and 604711), the Innovation and Technology Commission (ITP/008/09NP), the University Grants Committee of Hong Kong (AoE/P-03/08), the NSFC/RGC grant (N_HKUST620/11), and the National Science Foundation of China (21104044, 20974028, 21074073).

REFERENCES

- (1) (a) *Physical Properties of Liquid Crystals*; Demus, D., Gooby, J. W., Gray, G. W., Spiess, H. W., Vill, V., Eds.; Wiley-VCH: Weinheim, Germany, 1999. (b) *Liquid Crystalline Polymer Systems*; Isayev, A. I., Kyu, T., Cheng, S. Z. D., Eds.; American Chemical Society: Washington, DC, 1996.
- (2) (a) Kato, T.; Mizoshita, N.; Kishimoto, K. *Angew. Chem., Int. Ed.* **2006**, *45*, 38. (b) Donald, A. M.; Windle, A. H.; Hanna, S. *Liquid Crystalline Polymers*, 2nd ed.; Cambridge University Press: Cambridge, U.K., 2006.
- (3) Weder, C.; Sarwa, C.; Montali, A.; Bastiaansen, C.; Smith, P. *Science* **1998**, *279*, 835.
- (4) Moreira, M. F.; Carvalho, I. C. S.; Cao, W.; Bailey, C.; Taheri, B.; Palffy-Muhoray, P. *Appl. Phys. Lett.* **2004**, *85*, 2691.
- (5) Yablonskii, S. V.; Nakano, K.; Mikhailov, A. S.; Ozaki, M.; Yoshino, K. *Appl. Phys. Lett.* **2002**, *80*, 571.
- (6) (a) Schadt, M. *Liq. Cryst.* **1993**, *14*, 73. (b) Suda, K.; Akagi, K. *J. Polym. Sci., Part A: Polym. Chem.* **2008**, *46*, 3591.

- (7) (a) Shimizu, Y.; Monobe, H.; Heinrich, B.; Guillon, D.; Oikawa, K.; Nakayama, K. *Mol. Cryst. Liq. Cryst.* **2009**, *509*, 948. (b) Funahashi, M. *Polym. J.* **2009**, *41*, 459. (c) McCulloch, I.; Heeney, M.; Bailey, C.; Genevicius, K.; MacDonald, I.; Shkunov, M.; Sparrowe, D.; Tierney, S.; Wagner, R.; Zhang, W.; Chabinyi, M. L.; Kline, R. J.; McGehee, M. D.; Toney, M. F. *Nat. Mater.* **2006**, *5*, 328.
- (8) (a) Sun, Q.; Park, K.; Dai, L. *J. Phys. Chem. C* **2009**, *113*, 7892. (b) Li, L.; Kang, S.-W.; Harden, J.; Sun, Q.; Zhou, X.; Dai, L.; Jakli, A.; Kumar, S.; Li, Q. *Liq. Cryst.* **2008**, *35*, 233. (c) Huang, W. Y.; Huang, P. T.; Han, Y. K.; Lee, C. C.; Hsieh, T. L.; Chang, M. Y. *Macromolecules* **2008**, *41*, 7485.
- (9) (a) Lüssem, G.; Wendorff, J. H. *Polym. Adv. Technol.* **1998**, *9*, 443. (b) Whitehead, K. S.; Grell, M.; Bradley, D. D. C.; Inbasekaran, M.; Woo, E. P. *Synth. Met.* **2000**, *111–112*, 181.
- (10) (a) Adam, D.; Schuhmacher, P.; Simmerer, J.; Häussling, L.; Siemensmeyer, K.; Etzbach, K. H.; Ringsdorf, H.; Haarer, D. *Nature* **1994**, *371*, 141. (b) Percec, V.; Glodde, M.; Bera, T. K.; Miura, Y.; Shiyannovskaya, I.; Singer, K. D.; V. Balagurusamy, S. K.; Heiney, P. A.; Schnell, L.; Rapp, A.; Spiess, H.-W.; Hudson, S. D.; Duan, H. *Nature* **2002**, *419*, 384. (c) Xiao, S.; Myers, M.; Miao, Q.; Sanaur, S.; Pang, K.; Steigerwald, M. L.; Nuckolls, C. *Angew. Chem., Int. Ed.* **2005**, *44*, 7390. (d) Hirai, Y.; Monobe, H.; Mizoshita, N.; Moriyama, M.; Hanabusa, K.; Shimizu, Y.; Kato, T. *Adv. Funct. Mater.* **2008**, *18*, 1668. (e) Hassheider, T.; Benning, S. A.; Kitzerow, H.-S.; Achard, M.-F.; Bock, H. *Angew. Chem., Int. Ed.* **2001**, *40*, 2060.
- (11) (a) Yoshio, M.; Mukai, T.; Ohno, H.; Kato, T. *J. Am. Chem. Soc.* **2004**, *126*, 994. (b) Cho, B.-K.; Jain, A.; Gruner, S. M.; Wiesner, U. *Science* **2004**, *305*, 1598. (c) Ichikawa, T.; Yoshio, M.; Hamasaki, A.; Mukai, T.; Ohno, H.; Kato, T. *J. Am. Chem. Soc.* **2007**, *129*, 10662.
- (12) Zhou, M.; Kidd, T. J.; Noble, R. D.; Gin, D. L. *Adv. Mater.* **2005**, *17*, 1850.
- (13) (a) Yasuda, T.; Ooi, H.; Morita, J.; Akama, Y.; Minoura, K.; Funahashi, M.; Shimomura, T.; Kato, T. *Adv. Funct. Mater.* **2009**, *19*, 411. (b) Zhu, Z.; Swager, T. M. *J. Am. Chem. Soc.* **2002**, *124*, 9670. (c) Wang, H.; Zhang, F.; Bai, B.; Zhang, P.; Shi, J.; Yu, D.; Zhao, Y.; Wang, Y.; Li, M. *Liq. Cryst.* **2008**, *35*, 905. (d) Li, X.; Liu, A.; Xun, S.; Qiao, W.; Wan, X.; Wang, Z. Y. *Org. Lett.* **2008**, *10*, 3785. (e) de Halleux, V.; Calbert, J.-P.; Brocorens, P.; Cornil, J.; Declercq, J.-P.; Brédas, J.-L.; Geerts, Y. *Adv. Funct. Mater.* **2004**, *14*, 649. (f) Li, X.-Q.; Zhang, X.; Ghosh, S.; Würthner, F. *Chem.—Eur. J.* **2008**, *14*, 8074. (g) Conger, B. M.; Mastrangelo, J. C.; Chen, S. H. *Macromolecules* **1997**, *30*, 4049. (h) Olivier, J.-H.; Camerel, F.; Ulrich, G.; Barberá, J.; Ziessel, R. *Chem.—Eur. J.* **2010**, *16*, 7134.
- (14) (a) Camerel, F.; Bonardi, L.; Schmutz, M.; Ziessel, R. *J. Am. Chem. Soc.* **2006**, *128*, 4548. (b) Yelamaggad, C. V.; Achalkumar, A. S.; Rao, D. S. S.; Prasad, S. K. *J. Org. Chem.* **2009**, *74*, 3168. (c) Yang, C.-W.; Hsia, T.-H.; Chen, C.-C.; Lai, C.-K.; Liu, R.-S. *Org. Lett.* **2008**, *10*, 4069. (d) Binnemans, K. *J. Org. Chem.* **2009**, *74*, 3168. (e) Sagara, Y.; Kato, T. *Angew. Chem., Int. Ed.* **2008**, *47*, 5175. (f) Davey, A. P.; Howard, R. G.; Blau, W. J. *J. Mater. Chem.* **1997**, *7*, 417. (g) Molard, Y.; Dorson, F.; Cîrcu, V.; Roisnel, T.; Artzner, F.; Cordier, S. *Angew. Chem., Int. Ed.* **2010**, *49*, 3351. (h) Hayer, A.; de Halleux, V.; Kohlher, A.; El-Garoughy, A.; Meijer, E. W.; Barberá, J.; Tant, J.; Levin, J.; Lehmann, M.; Gierschner, J.; Cornil, J.; Geerts, Y. H. *J. Phys. Chem. B* **2006**, *110*, 7653. (i) Li, C.-Z.; Matsuo, Y.; Nakamura, E. *J. Am. Chem. Soc.* **2009**, *131*, 17058. (j) Pérez, A.; Serrano, J. L.; Sierra, T.; Ballesteros, A.; de Saá, D.; Barluenga, J. *J. Am. Chem. Soc.* **2011**, *133*, 8110. (k) Liao, C.-T.; Chen, H.-H.; Hsu, H.-F.; Anurach Poloek, A.; Yeh, H.-H.; Chi, Y.; Wang, K.-W.; Lai, C.-H.; Lee, G.-H.; Shih, C.-W.; Chou, P.-T. *Chem.—Eur. J.* **2011**, *17*, 546.
- (15) (a) Vijayaraghavan, R. K.; Abraham, S.; Akiyama, H.; Furumi, S.; Tamaoki, N.; Das, S. *Adv. Funct. Mater.* **2008**, *18*, 2510. (b) Seo, J.; Kim, S.; Gihm, S. H.; Park, C. R.; Park, S. Y. *J. Mater. Chem.* **2007**, *17*, 5052.
- (16) (a) Beer, A.; Scherowsky, G.; Owen, H.; Coles, H. *Liq. Cryst.* **1995**, *19*, 565. and references therein. (b) Christ, T.; Glusen, B.; Greiner, A.; Kettner, A.; Sander, R.; Stumpfen, V.; Tsukruk, V.; Wendorff, J. H. *Adv. Mater.* **1997**, *9*, 48.
- (17) (a) Grell, M.; Bradley, D. D. C. *Adv. Mater.* **1999**, *11*, 895. (b) Hayasaka, H.; Tamura, K.; Akagi, K. *Macromolecules* **2008**, *41*, 2341. (c) Hayasaka, H.; Miyashita, T.; Tamura, K.; Akagi, K. *Adv. Func. Mater.* **2010**, *20*, 1243. (d) Jeong, Y. S.; Akagi, K. *J. Mater. Chem.* **2011**, *21*, 10472. (e) San Jose, B. A.; Matsushita, S.; Moroishi, Y.; Akagi, K. *Macromolecules* **2011**, *44*, 6288. (f) *Handbook of Thiophene-Based Materials: Applications in Organic Electronics and Photonics*; Perepichka, I. F., Perepichka, D. F., Eds.; John Wiley Sons: New York, 2009; Chapter 12, pp 497–515. (g) *Thermotropic Liquid Crystals: Recent Advances*; Ramamoorthy, A., Ed.; Springer: Dordrecht, The Netherlands, 2007; Chapter 9, pp 249–275.
- (18) Chen, S. H.; Shi, H.; Conger, B. M.; Mastrangelo, J. C.; Tsutsui, T. *Adv. Mater.* **1996**, *8*, 998.
- (19) Birks, J. B. *Photophysics of Aromatic Molecules*; Wiley: London, 1970.
- (20) Ting, C.-H.; Chen, J.-T.; Hsu, C.-S. *Macromolecules* **2002**, *35*, 1180.
- (21) Jenekhe, S. A.; Osaheni, J. A. *Science* **1994**, *265*, 765.
- (22) (a) Lam, J. W. Y.; Tang, B. Z. *J. Polym. Sci., Part A: Polym. Chem.* **2003**, *41*, 2607. (b) Lam, J. W. Y.; Tang, B. Z. *Acc. Chem. Res.* **2005**, *38*, 745. (c) Kong, X.; Lam, J. W. Y.; Tang, B. Z. *Macromolecules* **1999**, *32*, 1722. (d) Liu, J.; Lam, J. W. Y.; Tang, B. Z. *Chem. Rev.* **2009**, *109*, 5799.
- (23) (a) Lam, J. W. Y.; Dong, Y.; Tang, B. Z. *Macromolecules* **2002**, *35*, 8288. (b) Lam, J. W. Y.; Qin, A.; Dong, Y.; Lai, L. M.; Haessler, M.; Dong, Y.; Tang, B. Z. *J. Phys. Chem. B* **2006**, *110*, 21613. (c) Lam, J. W. Y.; Dong, Y.; Cheuk, K. K. L.; Luo, J.; Xie, Z.; Kwok, H. S.; Mo, Z.; Tang, B. Z. *Macromolecules* **2002**, *35*, 1229. (d) Huang, Y. M.; Lam, J. W. Y.; Cheuk, K. K. L.; Ge, W.; Tang, B. Z. *Mater. Sci. Eng., B* **2001**, *85*, 242.
- (24) Yuan, W. Z.; Lam, J. W. Y.; Shen, X. Y.; Sun, J. Z.; Mahtab, F.; Zheng, Q.; Tang, B. Z. *Macromolecules* **2009**, *42*, 2523.
- (25) (a) Luo, J.; Xie, Z.; Lam, J. W. Y.; Cheng, L.; Chen, H.; Qiu, C.; Kwok, H. S.; Zhan, X.; Liu, Y.; Zhu, D.; Tang, B. Z. *Chem. Commun.* **2001**, 1740. (b) Chen, J.; Law, C. C. W.; Lam, J. W. Y.; Dong, Y.; Lo, S. M. F.; Williams, I. D.; Zhu, D.; Tang, B. Z. *Chem. Mater.* **2003**, *15*, 1535. (c) Zeng, Q.; Li, Z.; Dong, Y.; Di, C.; Qin, A.; Hong, Y.; Ji, L.; Zhu, Z.; Jim, C. K. W.; Yu, G.; Li, Q.; Li, Z.; Liu, Y.; Qin, J.; Tang, B. Z. *Chem. Commun.* **2007**, 70. (d) Li, Z.; Dong, Y.; Mi, B.; Tang, Y.; Häussler, M.; Tong, H.; Dong, Y.; Lam, J. W. Y.; Ren, Y.; Sung, H. H. Y.; Wong, K. S.; Gao, P.; Williams, I. D.; Kwok, H. S.; Tang, B. Z. *J. Phys. Chem. B* **2005**, *109*, 10061.
- (26) For reviews, see: (a) Hong, Y.; Lam, J. W. Y.; Tang, B. Z. *Chem. Commun.* **2009**, 4332. (b) Liu, J.; Lam, J. W. Y.; Tang, B. Z. *J. Inorg. Organomet. Polym. Mater.* **2009**, *19*, 249.
- (27) (a) Tong, H.; Hong, Y.; Dong, Y.; Häussler, M.; Li, Z.; Lam, J. W. Y.; Dong, Y.; Sung, H. H.-Y.; Williams, I. D.; Tang, B. Z. *J. Phys. Chem. B* **2007**, *111*, 11817. (b) Dong, Y.; Lam, J. W. Y.; Qin, A.; Liu, J.; Li, Z.; Tang, B. Z.; Sun, J.; Kwok, H. K. *Appl. Phys. Lett.* **2007**, *91*, 011111.
- (28) (a) Yuan, W. Z.; Zhao, H.; Shen, X. Y.; Mahtab, F.; Lam, J. W. Y.; Sun, J. Z.; Tang, B. Z. *Macromolecules* **2009**, *42*, 9400. (b) Qin, A.; Lam, J. W. Y.; Tang, L.; Jim, C. K. W.; Zhao, H.; Sun, J.; Tang, B. Z. *Macromolecules* **2009**, *42*, 1421.
- (29) Kolb, H. C.; Finn, M. G.; Sharpless, K. B. *Angew. Chem. Int. Ed.* **2001**, *40*, 2004.
- (30) Lodge, T. P. *Macromolecules* **2009**, *42*, 3827 and references therein.
- (31) (a) Binder, W. H.; Sachsenhofer, R. *Macromol. Rapid Commun.* **2008**, *29*, 952. (b) Johnson, J. A.; Finn, M. G.; Koberstein, J. T.; Turro, N. J. *Macromol. Rapid Commun.* **2008**, *29*, 1052. (c) Nandivada, H.; Jiang, X.; Lahann, J. *Adv. Mater.* **2007**, *19*, 2197. (d) Moses, J. E.; Moorhouse, A. D. *Chem. Soc. Rev.* **2007**, *36*, 1249. (e) Fournier, D.; Hoogenboom, R.; Schubert, U. S. *Chem. Soc. Rev.* **2007**, *36*, 1369. (f) Goodall, G. W.; Hayes, W. *Chem. Soc. Rev.* **2006**, *35*, 280. (g) Qin, A.; Lam, J. W. Y.; Tang, B. Z. *Macromolecules* **2010**, *43*, 8693. (h) Qin, A.; Lam, J. W. Y.; Tang, B. Z. *Chem. Soc. Rev.* **2010**, *39*, 2522.
- (32) (a) Gujadhur, R.; Venkataraman, D.; Kintigh, J. T. *Tetrahedron Lett.* **2001**, *42*, 4791. (b) Liu, J.; Zhang, L.; Lam, J. W. Y.; Jim, C. K. W.;

Yue, Y.; Deng, R.; Hong, Y.; Qin, A.; Sung, H. H. Y.; Williams, I. D.; Jia, G.; Tang, B. Z. *Macromolecules* **2009**, *42*, 7367.

(33) Qin, A.; Lam, J. W. Y.; Jim, C. K. W.; Zhang, L.; Yan, J.; Häußler, M.; Liu, J.; Dong, Y.; Liang, D.; Chen, E.; Jia, G.; Tang, B. Z. *Macromolecules* **2008**, *41*, 3808.

(34) Brandrup, J.; Immergut, E. H., Grulke, E. A., Eds.; *Polymer Handbook*, 4th Ed.; Wiley: New York, 1999.

(35) (a) Gray, G. W.; Goodby, J. W. G. *Smectic Liquid Crystals: Texture and Structures*; Leonard Hill: London, 1984. (b) Demus, D.; Richter, L. *Textures of Liquid Crystals*; Verlag Chemie: Weinheim, Germany, 1978.

(36) (a) Ye, C.; Zhang, H.-L.; Huang, Y.; Chen, E.-Q.; Lu, Y.; Shen, D.; Wan, X.-H.; Shen, Z.; Cheng, S. Z. D.; Zhou, Q.-F. *Macromolecules* **2004**, *37*, 7188. (b) Liu, A.; Zhi, J.; Cui, J.; Wan, X.; Zhou, Q. *Macromolecules* **2007**, *40*, 8233. (c) Guan, Y.; Chen, X.; Shen, Z.; Wan, X.; Zhou, Q. *Polymer* **2009**, *50*, 936.

(37) (a) Yoon, Y.; Ho, R. M.; Li, F. M.; Leland, M. E.; Park, J. Y.; Cheng, S. Z. D.; Percec, V.; Chu, P. *Prog. Polym. Sci.* **1997**, *22*, 765. (b) Ungar, G.; Feijoo, J. L.; Keller, A.; Yourd, R.; Percec, V. *Macromolecules* **1990**, *23*, 3411. (c) Yandrasits, M. A.; Cheng, S. Z. D.; Zhang, A. Q.; Cheng, J. L.; Wunderlich, B.; Percec, V. *Macromolecules* **1992**, *25*, 2112. (d) Pardey, R.; Harris, F. W.; Cheng, S. Z. D.; Aducci, J.; Facinelli, J. V.; Lenz, R. W. *Macromolecules* **1993**, *26*, 3687.